Frontiers in Heat and Mass Transfer (FHMT), 20, 27 (2023)
DOI: 10.5098/hmt.20.27

Global Digital Central
ISSN: 2151-8629

**Frontiers in Heat and Mass Transfer**

Available at www.ThermalFluidsCentral.org

# CONVECTIVE HEAT EXCHANGER FROM RENEWABLE SUN RADIATION BY NANOFLUIDS FLOW IN DIRECT ABSORPTION SOLAR COLLECTORS WITH ENTROPY

Girma Tafesse[†], Mitiku Daba , Vedagiri G. Naidu

*Department of Applied Mathematics, School of Applied Natural Science, Adama Science and Technology University, Adama, Post Box: 1888, Ethiopia*

**ABSTRACT**

Innovative technologies necessitate extra energy, which can be captured from environmentally sustainable, renewable solar energy. Here, heat and mass transfer through stirring nanofluids in solar collectors for direct absorption of sunlight are pronounced. The similarity transformation served to turn mathematically regulated partial differential equations into sets of nonlinear higher-order ordinary differential equations. These equations have been resolved by the homotopy analysis method manipulating, BVPh2.0 package in Mathematica 12.1. Validations are justified through comparison. Afterward, stronger magnetic field interactions delay the nanofluids mobility. Temperature increases with thermal radiation and Biot numbers. Entropy formation and nanoparticle concentration dwindle when Schmidt's number surges.

**Keywords**: *Energy, Thermal Transfer, Micro-sized particle, Energy loss, Homotopy Analysis Method.*

## 1. INTRODUCTION

The ultimate need of people in the world mostly accomplished by consuming energy and thus, the role of energy has been uncountable in our day to days activities. Based on the Central Statistics Office report (Statistics, 2016), the usage of non-renewable energy like coal, fossil fuel in many industries, convey system, residential, agricultural and educational sectors are increasing from month to months. In these kind of utilization, there have been a bulky amount of carbon dioxide released which leads to alter the existing climate and cause global warming (Szulejko *et al.*, 2017). As a result of uprising the importance of energy, it is a crucial work to find viable, clean and unlimited energy source called renewable energy. Dincer (2000) suggested that the renewable energy is preferable since it has no consequence effect to the environment which abolishes the disadvantage of non-renewable energy. Henceforth, operating renewable energy on our work, nullify the environmental challenge inline with the high demand of energy and rapid economical growth as Lei *et al.* (2022) stated. Some sources of renewable energy are biomass, geothermal, wave, tidal, nuclear energy, solar energy, wind energy and water energy (Tiwari and Mishra, 2012; Panwar *et al.*, 2011; Everett *et al.*, 2012). However, they have some demerits on practical implementations, such as high initial cost, hard to produce large amount, need wide area on earth, and consistence on supplement (Bhalla and Tyagi, 2018). But, for the merits of renewable energy, academics are now hypnotized by it to lessen the world's economic and climatic crises. As well, the sustainability and adequacy of energy assured by renewable energy. For example, solar energy is suitable for the environment, acceptable and obtained everyplace in abundant (Bayrak *et al.*, 2017). Recently, Flilihi *et al.* (2022) declared that, it is used for sundry industrial operations, like indirect solar dryer, plus warming homes and generating local hot water. Sathyamurthy *et al.* (2014) also underlined the financial benefits of solar stills.

In general, to make our life easy using the modern technology, energy is required at any time and in large amount. For these, solar energy is recommended which is naturally replaceable and environmentally friendly. As an example, consider smart mobile phones which is important to read, talk and attend videos, write on it, and play game, operate with enough amount of energy daily. Therefore, collecting solar radiation adequately, satisfy the demand of energy. As a matter of fact, many scientists focused their attention towards upgrading the effective collection and using solar energy (Sabiha *et al.*, 2015; Pandey and Chaurasiya, 2017; Rasih *et al.*, 2019; Flilihi *et al.*, 2022). Bhalla and Tyagi (2018) stated that there are two mechanisms of gathering solar energy.

1. Solar photovoltaic cells: Using semiconductor cell, these mechanism alter energy from sun into electric power directly by solar panels and produce electricity (Al-Waeli *et al.*, 2017; Sathe and Dhoble, 2017).

2. Solar thermal collectors: In these, the solar energy induce electricity after bringing it into mechanical energy. They can be applied for different purposes such as heating/cooling process, steam generation, electric power production etc (Gorji and Ranjbar, 2017).

Bhalla and Tyagi (2018) noted that practically the solar thermal collectors have greater potential of harvesting sun's radiation than solar photovoltaic cell. The solar thermal collector can be classified as concentrated which gives energy from the solar radiation via transport medium and

[†]*Corresponding Author. Email: girmat1@gmail.com*

Global Digital Central
ISSN: 2151-8629

non-concentrated solar collector where we use energy directly for industry, endemic water heating, solar space heating, and equipment for washing air and controlling humidity (Gorji and Ranjbar, 2017; Rasih *et al.*, 2019). As Rasih *et al.* (2019) deliberated, the sun's radiation collected and transpose into heat via absorber. Then using working fluid, the heat energy converted into another form of energy called indirect absorption solar collector (IASC). However, the failure of IASC is to sustain high temperature which is very important to collect more solar radiation. The idea of direct absorption solar collector (DASC) began by Minardi and Chuang (1975) which nullify the complain on IASC. In DASC, there is a straight relation between the sun's radiation and transport medium without any interface which detracts the loss of solar energy due to convection and conduction (Dugaria *et al.*, 2018).

Nanofluids can be defined as a microscopic particle that exist in the base fluid such as water, ethanol, oil whose size measured by nano meter. The idea of nanofluids first fired by Choi and Eastman (1995) and presented on the their thermophysical features such as thermal conductivity, thermal diffusivity, viscosity, and convective heat-transfer coefficients. They concluded that, adding nanofluids to base fluid amended the thermophysical characters due to the motion of nano-sized particles in the conventional basic fluids. These advancements could assist heat and mass transfer, the building of energy-efficient structures, the usage of solar collectors, biomedical applications, and other engineering uses (Wakif *et al.*, 2018). Thus, most scientists aspired towards the application of nanofluids, particularly with respect to heat transfer in solar collectors and they remarked that, the effectiveness of solar collector upgraded using nanofluids (Subramani *et al.*, 2018; Bhalla and Tyagi, 2017; Maouassi *et al.*, 2018). Beside, numerous researchers have illuminated the transmission of heat from non polluting renewable solar energy through nanofluids flow. For instance, Azam *et al.*, 2019 revised time dependent convective flow of magnetohydrodynamic (MHD) cross nanofuid with respect to solar energy numerically. The cause of heat exploration from renewable sun's radiation in a parabolic trough solar collector (PTSC) upon Maxwell nanofluid was examined by Jamshed *et al.* (2021). Numerically, using Keller box technique they compared the heat transfer of the two different types of nanofluids. Alkathiri *et al.* (2022) also elaborated this idea using Galerkin finite element method and tested the heat expansion on renewable solar energy within the binary nanofluid in PTSC.

Entropy can be defined as the approximation of disorder change from order. It is the hottest issue relating to the analysis of heat transfer and designing the minimum production based on second law of thermodynamics. Bejan (1996) was the beginner on concepts of entropy. Total entropy affected by fluid viscosity, mass and heat exchange irreversibilities. As Tyagi *et al.* (2007) stated, the production of irreversibility leads to decrease the existing work. Thus, intentionally an add on energy from sun's radiation lowers the work done. Achievement of collecting energy from solar collector needs enhancement by adopting the second law analysis-based scheme (Smit and Kessels, 2015). Different studies explained the generation of entropy based on heat irreversibility or conduction impact, friction flow of fluid, hydromagnetic effect, mass, porosity irreversibility, dissipation irreversibility and Joule heat on various kinds of nanofluids Aziz *et al.* (2018); Daniel *et al.* (2017); Hayat *et al.* (2019); Loganathan *et al.* (2021). From these inquiries, the total entropy increase with respect to parameter like temperature difference, Brinkman number, porosity, radiation and magnetic parameters.

Based on the latest research work, there is a limited information on the mathematical analysis of convective heat exchanger from liable plenteous solar energy through nanofluids in DASC with entropy procreation using semi-analytic approach called homotopy analysis method (HAM). HAM capable of achieving a series solutions for boundary value problem of nonlinear higher-order systems of ordinary differential equations nicely. As far as the information we have, such problem has not yet noted. Thus, the researchers aspired to overlook the transfer of sun's radiation directly to nanofluids as a transporting medium and analyzing the entropy generation by considering the flow, temperature and concentration of the nano-sized particle. By including these points, the obtained equations are solved by an extensively recognized analytic approach called HAM, coded by BVPh2.0 package on Mathematica 12.1 software.

## 2. MATHEMATICAL FORMULATION

In this problem, the rectangular coordinate system has been supposed and the surface begin stretching at $t > 0$ like Hussain *et al.* (2015). Then, the plate elongated horizontally with non uniform velocity, temperature and concentration having the following formulae at the sheet wall.

$$U_w = \frac{\mathfrak{B}x}{1-\varsigma t}, \bar{T}_w = \bar{T}_\infty + \frac{\bar{T}_0 \mathfrak{B}x^2}{\nu(1-\varsigma t)} \text{ and } \bar{C}_w = \bar{C}_\infty + \frac{\bar{C}_0 \mathfrak{B}x^2}{\nu(1-\varsigma t)} \tag{1}$$

Thus, $\bar{T}_0$ and $\bar{C}_0$ are constants, $U_w$, $\bar{T}_w$ and $\bar{C}_w$ denote the plate velocity, temperature, and nanoparticle concentration at the wall, in that order; $\mathfrak{B}$ and $\frac{\mathfrak{B}}{1-\varsigma t}$ are the starting and effective extending rates of the plate, respectively where $\mathfrak{B}$ and $\varsigma$ are non negative constants having $(\text{time})^{-1}$ unit. The flow of this model set out on Fig. 1 to give an imaginative image about the contemplated problem.

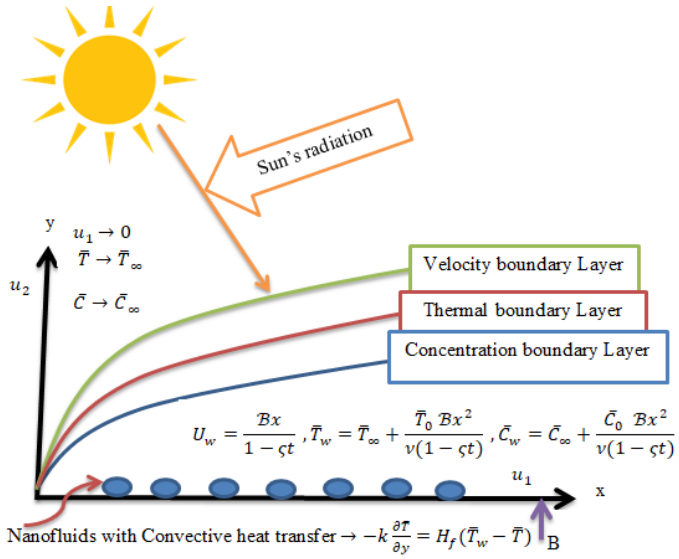


**Fig. 1** The physical schematic flow diagram

The basic assumptions for the flow model are listed as follows.

- Two dimensional incompresssible unsteady flows.
- Applying Boundary-layer approximations.
- Mixing nano-sized particle on base fluid.
- Considering Buongiorno model (Buongiorno, 2006) where the impact of Brownian motion and thermophoresis are weighed.
- Effect of solar radiation directly on flow of nanofluid.
- Flow having viscous dissipation properties and energy loss.
- Induced magnetic field is insignificant due to the low magnetic Reynolds number.

Global Digital Central
ISSN: 2151-8629

### 2.1. The Basic Governing Equations

The fundamental governing equations on the conservation of mass, momentum, energy, and nanoparticle volume fraction can be derived as Hussain *et al.* (2015); Kebede *et al.* (2020); Hussain (2022).

$$\frac{\partial u_1}{\partial x}+\frac{\partial u_2}{\partial y}=0 \tag{2}$$

$$\frac{\partial u_1}{\partial t}+u_1\frac{\partial u_1}{\partial x}+u_2\frac{\partial u_1}{\partial y}=\nu\frac{\partial^2 u_1}{\partial y^2}-\frac{\sigma_e B_0^2 u_1}{\rho(1-\varsigma t)} \tag{3}$$

$$\begin{aligned}\frac{\partial \bar{T}}{\partial t}+u_1\frac{\partial \bar{T}}{\partial x}+u_2\frac{\partial \bar{T}}{\partial y}=&\frac{k}{\rho c_p}\frac{\partial^2 \bar{T}}{\partial y^2}+\frac{\mu}{\rho c_p}(\frac{\partial u_1}{\partial y})^2-\frac{1}{\rho c_p}\frac{\partial q_r}{\partial y}\\&+\tau\left(D_B\frac{\partial \bar{C}}{\partial y}\frac{\partial \bar{T}}{\partial y}+\frac{D_T}{T_\infty}(\frac{\partial \bar{T}}{\partial y})^2\right)\end{aligned} \tag{4}$$

$$\frac{\partial \bar{C}}{\partial t}+u_1\frac{\partial \bar{C}}{\partial x}+u_2\frac{\partial \bar{C}}{\partial y}=D_B\frac{\partial^2 \bar{C}}{\partial y^2}+\frac{D_T}{T_\infty}\frac{\partial^2 \bar{T}}{\partial y^2} \tag{5}$$

The related boundary condition for this model from Aziz *et al.* (2021) and Ullah *et al.* (2017) work, we have

$$\begin{aligned}&\text{For } y=0; u_2=0, u_1=U_w, -k\frac{\partial \bar{T}}{\partial y}=H_f(\bar{T}_w-\bar{T}), \bar{C}=\bar{C}_w\\&\text{and } y\to\infty; u_1\to 0, \bar{T}\to\bar{T}_\infty, \bar{C}\to\bar{C}_\infty\end{aligned} \tag{6}$$

For minor difference in temperature between the sheet and around the nanofluids, we can apply the Rosseland-approximation to describe radiative term on Eq. (4). Thus by Kebede *et al.* (2020) and Brewster (1992), we have

$$q_r=-\frac{4\sigma^*}{k^*}\frac{\partial(\bar{T}^4)}{\partial y}\approx-\frac{16\bar{T}_\infty^3\sigma^*}{3k^*}\frac{\partial \bar{T}}{\partial y} \tag{7}$$

Thus, Eq. (4) reduced as

$$\begin{aligned}\frac{\partial \bar{T}}{\partial t}+u_1\frac{\partial \bar{T}}{\partial x}+u_2\frac{\partial \bar{T}}{\partial y}=&\frac{k}{\rho c_p}\left(1+\frac{16\bar{T}_\infty^3\sigma^*}{3k^*k}\right)\frac{\partial^2 \bar{T}}{\partial y^2}+\frac{\mu}{\rho c_p}(\frac{\partial u_1}{\partial y})^2\\&+\tau\left(D_B\frac{\partial \bar{C}}{\partial y}\frac{\partial \bar{T}}{\partial y}+\frac{D_T}{T_\infty}(\frac{\partial \bar{T}}{\partial y})^2\right)\end{aligned} \tag{8}$$

For mathematical analysis purpose, the partial differential Eqs. (2), (3), (5) and (8) have been recast into ordinary differential equations (ODEs) by launching a similarity transformation variable with stream function $\psi$ and dimensionless independent variable $\xi$ defined as follows.

$$\xi=y\sqrt{\frac{\mathfrak{B}}{\nu(1-\varsigma t)}}, \psi(x,y,t)=\sqrt{\frac{\mathfrak{B}\nu}{1-\varsigma t}}xF(\xi) \tag{9}$$

Using Eq. (9), the velocity components $u_1$ and $u_2$, temperature $\bar{T}$ and concentration $\bar{C}$ have been expressed in dimensionless form as follows:

$$\begin{aligned}&u_1(\xi)=\frac{\partial\psi}{\partial y}=\frac{\mathfrak{B}x}{1-\varsigma t}\frac{\partial F}{\partial\xi}, u_2(\xi)=-\frac{\partial\psi}{\partial x}=-\sqrt{\frac{\mathfrak{B}\nu}{1-\varsigma t}}F(\xi)\\&\Theta(\xi)=\frac{\bar{T}-\bar{T}_\infty}{\bar{T}_w-\bar{T}_\infty}, \Phi(\xi)=\frac{\bar{C}-\bar{C}_\infty}{\bar{C}_w-\bar{C}_\infty}\end{aligned} \tag{10}$$

Because of the continuous stream function $\psi$, Eq. (2) has been balanced. Then, the Eqs. (3), (5) and (8) have been modified in the following way.

$$F'''+FF''-A\left(F'+\frac{\xi}{2}F''\right)-(F')^2-MaF'=0 \tag{11}$$

$$\begin{aligned}&\frac{(1+Rn)}{Pr}\Theta''+Nb\Theta'\Phi'+Nt(\Theta')^2-A\left(\Theta+\frac{\xi}{2}\Theta'\right)-\Theta F'\\&+F\Theta'+Ec(F'')^2=0\end{aligned} \tag{12}$$

$$\Phi''-Sc\left[A\left(\Phi+\frac{\xi}{2}\Phi'\right)-F\Phi'+\Phi F'\right]+\frac{Nt}{Nb}\Theta''=0 \tag{13}$$

Correspondingly, boundary conditions in Eq. (6) become

$$\begin{aligned}&F(0)=0, F'(0)=1, \Theta'(0)=-\Upsilon(1-\Theta(0)), \Phi(0)=1\\&F'(\xi\to\infty)=0, \Theta(\xi\to\infty)=0, \Phi(\xi\to\infty)=0\end{aligned} \tag{14}$$

The obtained non dimensional arbitrary constants are $A=\frac{\varsigma}{\mathfrak{B}}$; unsteadiness parameter, $P_r=\frac{\nu\rho c_p}{k}$; Prandtl number, $Ma=\frac{\sigma_e B_0^2}{\mathfrak{B}\rho(1-\varsigma t)}$; magnetic interaction parameter, $Rn=\frac{16\sigma^*\bar{T}_\infty^3}{3kk^*}$; thermal radiation parameter, $N_b=\frac{D_B\tau(\bar{C}_w-\bar{C}_\infty)}{\nu}$; Brownian motion parameter, $N_t=\frac{D_T\tau(\bar{T}_w-\bar{T}_\infty)}{\bar{T}_\infty\nu}$; thermophoresis parameter. $Sc=\frac{\nu}{D_B}$; Schmidt number, $E_c=\frac{(U_w)^2}{(T_w-T_\infty)c_p}$; Eckert number and $\Upsilon=\frac{H_f}{k}\sqrt{\frac{\nu(1-\varsigma t)}{\mathfrak{B}}}$; Biot number.
The prime $'$ in Eqs. (11-13) pointed the differentiation with respect to $\xi$.

### 2.2. Physical Quantities in Engineering Perspective

In this portion, the three valuable physical quantities in the sight of engineering have been clarified depending on the supposed nanofluids.

1. Local skin friction or rate of momentum transfer ($Cf_x$) which interfere the flow of fluid over the surface and based on Rafique *et al.* (2019), we have

$$Cf_x=\frac{\tau_w}{\rho U_w^2}, \quad \text{where } \tau_w=\mu(\frac{\partial u_1}{\partial y})_{y=0} \tag{15}$$

In terms of non-dimensional variable, Eq. (15), becomes

$$Cf_x=\frac{\mu(\frac{\partial u_1}{\partial y})_{y=0}}{\rho U_w^2}=\frac{\mu(\frac{\partial^2\psi}{\partial y^2})_{y=0}}{\rho U_w^2}=Re_x^{-0.5}F''(0) \tag{16}$$

Where $Re_x=\frac{U_w x}{\nu}$ represents the local Reynolds number.

2. Local Nusslet number or rate of heat transfer ($Nu_x$) measure's the rate of heat transfer and defined as Kebede *et al.* (2020)

$$\begin{aligned}Nu_x=&-\frac{xk(\frac{\partial \bar{T}}{\partial y})_{y=0}}{k(\bar{T}-\bar{T}_\infty)}+\frac{q_r x}{k(\bar{T}-\bar{T}_\infty)}\\=&\left[\frac{-3k*k-16\bar{T}_\infty^4\sigma*}{3k*k(\bar{T}-\bar{T}_\infty)}\right]x\frac{\partial \bar{T}}{\partial y}_{y=0}\end{aligned} \tag{17}$$

Since $\bar{T}-\bar{T}_\infty=\bar{T}_w-\bar{T}_\infty$ at the surface ($y=0$), then Eq. (17) further simplified in the following manner.

$$Nu_x=-Re_x^{0.5}\left[1+Rn\right]\Theta'(0) \tag{18}$$

3. Sherwood number or mass transfer rate ($Sh_x$) is non-dimensional quantity applied on the mass transfer. According to Rafique *et al.* (2019), the equation of Sherwood number becomes

$$Sh_x=\frac{xJ_m}{D_B(\bar{C}_w-\bar{C}_\infty)}=-\frac{xD_B(\frac{\partial \bar{C}}{\partial y})_{y=0}}{D_B(\bar{C}_w-\bar{C}_\infty)}=-Re_x^{0.5}\Phi'(0) \tag{19}$$

Where $J_m=-D_B(\frac{\partial \bar{C}}{\partial y})_{y=0}$ assign for mass flux at $y=0$ of the plane.

Global Digital Central
ISSN: 2151-8629

### 2.3. Procreation of Entropy

To analyze and apply the solar energy properly, the concept of thermodynamic first and second law are essential. As Loganathan and Rajan (2020) stated, entropy is the disturbance of regular system and enclosing it which measure for not reversibility. With the existence of irreversible, it is tough to exchange the total solar radiation into heat, which minimizes the entire work done. Eventually, the researchers in this work accounted for the entropy formation triggered by heat transition, friction between nanofluids, and mass transmission. Based on Hussain (2022) and Loganathan and Rajan (2020), the formula of entropy has been modified as:

$$E_{pr} = \left\{ \frac{k}{\bar{T}_\infty^2} \left[ 1 + \frac{16\sigma^* \bar{T}_\infty^3}{3kk^*} \right] \left( \frac{\partial \bar{T}}{\partial y} \right)^2 \right\} + \left\{ \frac{\mu}{\bar{T}_\infty} \left( \frac{\partial u_1}{\partial y} \right)^2 \right\} + \left\{ \frac{RD}{\bar{C}_\infty} \left( \frac{\partial \bar{C}}{\partial y} \right)^2 + \frac{RD}{\bar{T}_\infty} \left( \frac{\partial \bar{C}}{\partial y} \right) \left( \frac{\partial \bar{T}}{\partial y} \right) \right\} \tag{20}$$

The non dimension form of local entropy ($NG$) in Eq. (20) can be done by multiplying the expression, $E_0 = \frac{\bar{T}_\infty^2 \mathfrak{B}^2}{k(\bar{T}_w - \bar{T}_\infty)^2}$. Thus, the dimensionless entropy ($NG = E_0 E_{pr}$) simplified using the Eq. (10) as

$$NG = Re(1+Rn)(\Theta')^2 + \frac{Re}{\Delta_1} \left[ Br(F'')^2 + \lambda_1 \Delta_2 \left( \Delta_2 (\Phi')^2 + \Phi' \Theta' \right) \right] \tag{21}$$

Where $Re = \frac{\mathfrak{B}^3}{\nu(1-\varsigma t)}$; global Reynolds number, $Br = \frac{\mu U_w^2}{k(\bar{T}_w - \bar{T}_\infty)}$; Brinkman number, $\Delta_1 = \frac{\bar{T}_w - \bar{T}_\infty}{\bar{T}_\infty}$; temperature difference, $\lambda_1 = \frac{RD\bar{C}_\infty}{k}$, diffusive variable and $\Delta_2 = \frac{\bar{C}_w - \bar{C}_\infty}{\bar{C}_\infty}$ concentration difference.

We have also Bejan number (Be) which is the ratio of entropy acquired by heat and mass transfer to the total entropy (Loganathan and Rajan, 2020). Mathematically, it can be stated as

$$Be = \frac{Re\Delta_1(1+Rn)(\Theta')^2 + Re\lambda_1\Delta_2 \left( \Delta_2 (\Phi')^2 + \Phi'\Theta' \right)}{\Delta_1 NG} \tag{22}$$

## 3. HOMOTOPY ANALYSIS METHOD

Currently, homotopy analysis method (HAM) is the best strategy to solve the boundary value problems in nonlinear higher-order system of ODEs. It was first forwarded by Liao in his PhD thesis (Liao, 1992). The series solutions using HAM are highly close to the exact one, which is why we call it a semi-analytic approach and most scholars put it into action. Some of the authors that apply HAM are Saeed *et al.* (2022); Hayat *et al.* (2021); Loganathan *et al.* (2021); Kebede *et al.* (2020); Bano *et al.* (2018). HAM have a great freedom to select convergence control parameters ($\hbar_F$, $\hbar_\Theta$ and $\hbar_\Phi$), initial guess ($F_0, \Theta_0$ and $\Phi_0$), auxiliary linear operators ($L_F$, $L_\Theta$ and $L_\Phi$) and auxiliary functions ($H_F(\xi)$, $H_\Theta(\xi)$, and $H_\Phi(\xi)$) to obtain an acceptable convergent solutions.

### 3.1. Electing Initial Guess, Linear Operators and Auxiliary Functions

The solution of Eqs. (11-13) likely to the exact answer by applying HAM.

- Initially, the solution of this problem approximated as

$$F_0 = 1 - e^{-\xi}, \quad \Theta_0 = \frac{\Upsilon e^{-\xi}}{1+\Upsilon}, \quad \text{and} \quad \Phi_0 = e^{-\xi} \tag{23}$$

- The appropriate auxiliary linear operators have been given below.

$$L_F = F''' - F', \quad L_\Theta = \Theta'' - \Theta, \quad \text{and} \quad L_\Phi = \Phi'' - \Phi \tag{24}$$

In this the linear operators meet the following relations.

$$L_F(C_1 + C_2 e^{\xi} + C_3 e^{-\xi}) = 0,$$
$$L_\Theta(C_4 e^{\xi} + C_5 e^{-\xi}) = 0$$
$$L_\Phi(C_6 e^{\xi} + C_7 e^{-\xi}) = 0$$

where $C_1 - C_7$ are constants to be determined based on the boundary conditions. Hence, $C_2 = C_4 = C_6 = 0$.

- Constant auxiliary functions have been picked for the dimensionless velocity, energy and nanoparticle concentrations which is:

$$H_F(\xi) = H_\Theta(\xi) = H_\Phi(\xi) = 1 \tag{25}$$

### 3.2. Zero$^{th}$ and m$^{th}$ order Deformation

For the non zero auxiliary parameter, $\hbar_F$, $\hbar_\Theta$ and $\hbar_\Phi$, the zeros order deformation defined as Kebede *et al.* (2020)

$$\begin{aligned}
(1-p)L_F[F(\xi;p) - F_0(\xi)] &= p\hbar_F H_F(\xi)\aleph_F[F(\xi;p)] \\
(1-p)L_\Theta[\Theta(\xi;p) - \Theta_0(\xi)] &= p\hbar_\Theta H_\Theta(\xi)\aleph_\Theta[F(\xi;p), \Theta(\xi;p), \Phi(\xi;p)] \\
(1-p)L_\Phi[\Phi(\xi;p) - \Phi_0(\xi)] &= p\hbar_\Phi H_\Phi(\xi)\aleph_\Phi[F(\xi;p), \Theta(\xi;p), \Phi(\xi;p)]
\end{aligned} \tag{26}$$

Where $p \in [0,1]$ is the homotopy embedding parameter without noticeable effect in this sense, $H_F$, $H_\Theta$ and $H_\Phi$ are auxiliary functions given in Eq. (25), and the nonlinear operators $\aleph_F$, $\aleph_\Theta$ and $\aleph_\Phi$ are defined in Eqs. (27), (28) and (29) below.

$$\begin{aligned}
\aleph_F[F(\xi;p)] =& \frac{\partial^3 F(\xi;p)}{\partial \xi^3} - A\left( \frac{\partial F(\xi;p)}{\partial \xi} + \frac{\xi}{2}\frac{\partial^2 F(\xi;p)}{\partial \xi^2} \right) \\
&+ F(\xi;p)\frac{\partial^2 F(\xi;p)}{\partial \xi^2} - \left( \frac{\partial F(\xi;p)}{\partial \xi} \right)^2 - Ma\frac{\partial F(\xi;p)}{\partial \xi}
\end{aligned} \tag{27}$$

$$\begin{aligned}
\aleph_\Theta[F(\xi;p), \Theta(\xi;p), \Phi(\xi;p)] =& \left(\frac{1+Rn}{Pr}\right)\frac{\partial^2 \Theta(\xi;p)}{\partial \xi^2} \\
&- A\left( \Theta(\xi;p) + \frac{\xi}{2}\frac{\partial \Theta(\xi;p)}{\partial \xi} \right) + Nt\left( \frac{\partial \Theta(\xi;p)}{\partial \xi} \right)^2 \\
&+ Nb\frac{\partial \Theta(\xi;p)}{\partial \xi}\frac{\partial \Phi(\xi;p)}{\partial \xi} + F(\xi;p)\frac{\partial \Theta(\xi;p)}{\partial \xi} \\
&- \Theta(\xi;p)\frac{\partial F(\xi;p)}{\partial \xi} + Ec\left( \frac{\partial^2 F(\xi;p)}{\partial \xi^2} \right)^2
\end{aligned} \tag{28}$$

$$\begin{aligned}
\aleph_\Phi[F(\xi;p), \Theta(\xi;p), \Phi(\xi;p)] =& \frac{\partial^2 \Phi(\xi;p)}{\partial \xi^2} + \frac{Nt}{Nb}\frac{\partial^2 \Theta(\xi;p)}{\partial \xi^2} \\
&+ Sc\left( F(\xi;p)\frac{\partial \Phi(\xi;p)}{\partial \xi} - \Phi(\xi;p)\frac{\partial F(\xi;p)}{\partial \xi} \right) \\
&- ScA\left( \Phi(\xi;p) + \frac{\xi}{2}\frac{\partial \Phi(\xi;p)}{\partial \xi} \right)
\end{aligned} \tag{29}$$

Next, the boundary conditions have been adjusted to:

$$\begin{aligned}
&F(0;p) = 0, \ \frac{\partial F(\xi;p)}{\partial \xi}|_{\xi=0} = 1, \ \left[ \frac{\partial \Theta(\xi;p)}{\partial \xi} \right]_{\xi=0} = \Upsilon(\Theta(0;p) - 1) \\
&\Phi(0;p) = 1, \ \frac{\partial F(\xi;p)}{\partial \xi}|_{\xi\to\infty} = \Phi(\xi;p)|_{\xi\to\infty} = \Phi(\xi;p)|_{\xi\to\infty} = 0
\end{aligned} \tag{30}$$

It is clear that when $p = 0$, $F(\xi,0) = F_0(\xi)$, $\Theta(\xi,0) = \Theta_0(\xi)$, and $\Phi(\xi,0) = \Phi_0(\xi)$ are solutions for the Eqs. (11-13). Likewise, at $p = 1$, the answer for these equations become $F(\xi,1) = F(\xi)$, $\Theta(\xi,1) = \Theta(\xi)$, and $\Phi(\xi,1) = \Phi(\xi)$. Thus, when the value of $p$ changes continuously

Global Digital Central
ISSN: 2151-8629

from 0 to 1, the homotopy solution also runs from initial guess $F_0(\xi)$, $\Theta_0(\xi)$, and $\Phi_0(\xi)$ to the accurate solution, $F(\xi)$, $\Theta(\xi)$, and $\Phi(\xi)$ according to Van Gorder (2014). As Rasheed *et al.* (2021) did, we expand using Taylor series expansion rule about $p = 0$, and hence we have:

$$F(\xi;p) = F_0(\xi) + \sum_{m=1}^{\infty} F_m(\xi)p^m, \Theta(\xi;p) = \Theta_0(\xi) + \sum_{m=1}^{\infty} \Theta_m(\xi)p^m$$
$$\Phi(\xi;p) = \Phi_0(\xi) + \sum_{m=1}^{\infty} \Phi_m(\xi)p^m, \tag{31}$$

In Eq. (31), $F_m(\xi)$, $\Theta_m(\xi)$, and $\Phi_m(\xi)$ can be defined as follows which are known as $m^{th}$ order homotopy derivative where $m \geq 1$.

$$F_m(\xi) = \frac{1}{m!}\frac{\partial^m F(\xi;p)}{\partial p^m}|_{p=0}, \Theta_m(\xi) = \frac{1}{m!}\frac{\partial^m \Theta(\xi;p)}{\partial p^m}|_{p=0}$$
$$\Phi_m(\xi) = \frac{1}{m!}\frac{\partial^m \Phi(\xi;p)}{\partial p^m}|_{p=0} \tag{32}$$

The $m^{th}$ order deformation obtained by differentiating the $0^{th}$ order Eq. (26) m-times with respect to $p$ and substituting the value of $p$ by zero, then dividing by $m$ factorial. Thus, the $m^{th}$ order deformation become:

$$L_F[F_m(\xi) - \chi_m F_{m-1}(\xi)] = \hbar_F H_F R^F_{m-1},$$
$$L_\Theta[\Theta_m(\xi) - \chi_m \Theta_{m-1}(\xi)] = \hbar_\Theta H_\Theta R^\Theta_{m-1}, \text{ and}$$
$$L_\Phi[\Phi_m(\xi) - \chi_m \Phi_{m-1}(\xi)] = \hbar_\Phi H_\Phi R^\Phi_{m-1} \tag{33}$$

Subject to the boundary conditions

$$F_m(0) = F'_m(0) = [\Theta'_m(0) + \Upsilon(1 - \Theta_m(0))] = \Phi_m(0) = 0$$
$$F'_m(\xi \to \infty) = \Theta_m(\xi \to \infty) = \Phi_m(\xi \to \infty) = 0 \tag{34}$$

Where a step function $\chi_m$ defined as

$$\chi_m = \begin{cases} 0, & \text{if } m \leq 1 \\ 1, & \text{if } m > 1 \end{cases} \tag{35}$$

In general $R^F_m$, $R^\Theta_m$ and $R^\Phi_m$ defined as

$$R^F_m = F'''_m + \sum_{l=0}^{m} F_l F''_{m-l} - A\left(F'_m + \frac{\xi}{2}F''_m\right) - \sum_{l=0}^{m} F'_l F'_{m-l} - MaF'_m \tag{36}$$

$$R^\Theta_m = \left(\frac{1+Rn}{Pr}\right)\Theta''_m - A\left(\Theta_m + \frac{\xi}{2}\Theta'_m\right) + Nb\sum_{l=0}^{m}\Theta'_l\Phi'_{m-l} + Nt\sum_{l=0}^{m}\Theta'_l\Theta'_{m-l} + \sum_{l=0}^{m}F_l\Theta'_{m-l} - \sum_{l=0}^{m}\Theta_l F'_{m-l} + Ec\sum_{l=0}^{m}F''_l F''_{m-l} \tag{37}$$

$$R^\Phi_m = \Phi''_m - Sc\left[A\left(\Phi_m + \frac{\xi}{2}\Phi'_m\right) - \sum_{l=0}^{m}F_l\Phi'_{m-l}\right] - Sc\sum_{l=0}^{m}\Phi_l F'_{m-l} + \frac{Nt}{Nb}\Theta''_m \tag{38}$$

To acquire the solution of Eqs. (11) to (13), we carry on the inverse linear operator on both sides of $m^{th}$ order deformation in Eq. (33). Thus, we got the following equations which have a repeating process.

$$F_m(\xi) = \chi_m F_{m-1}(\xi) + \hbar_F L_F^{-1}\sum H_F(\xi)R^F_{m-1}$$
$$\Theta_m(\xi) = \chi_m \Theta_{m-1}(\xi) + \hbar_\Theta L_\Theta^{-1}\sum H_\Theta(\xi)R^\Theta_{m-1}$$
$$\Phi_m(\xi) = \chi_m \Phi_{m-1}(\xi) + \hbar_\Phi L_\Phi^{-1}\sum H_\Phi(\xi)R^\Phi_{m-1} \tag{39}$$

In Eq. (39), for distinct individual value of $m = 1, 2, 3, ...$, we bring in a recurrence solution. Now we have an initial approximation $F_0(\xi)$, $\Theta_0(\xi)$ and $\Phi_0(\xi)$ from Eq. (23), auxiliary linear operator Eq. (24) and auxiliary function Eq. (25). Still the convergence control parameters $\hbar_F$, $\hbar_\Theta$ and $\hbar_\Phi$ are not specified. So, to get a convergent solution, we have the option of taking suitable convergence control parameters from the hiatus in $\hbar$-curves, and this is one benefit of HAM. This aids to achieve convergent solutions when $p = 1$ as seen below.

$$F(\xi;p) = F_0(\xi) + \sum_{m=1}^{\infty} p^m F_m(\xi) = F_0(\xi) + \sum_{m=1}^{\infty} F_m(\xi) = F(\xi)$$
$$\Theta(\xi;p) = \Theta_0(\xi) + \sum_{m=1}^{\infty} p^m \Theta_m(\xi) = \Theta_0(\xi) + \sum_{m=1}^{\infty} \Theta_m(\xi) = \Theta(\xi)$$
$$\Phi(\xi;p) = \Phi_0(\xi) + \sum_{m=1}^{\infty} p^m \Phi_m(\xi) = \Phi_0(\xi) + \sum_{m=1}^{\infty} \Phi_m(\xi) = \Phi(\xi) \tag{40}$$

### 3.3. Analyzing the Convergence

In HAM, the convergence of solutions mostly rely on the convergent control parameters. As Van Gorder (2014) discussed, the interval in which $\hbar$-curves are horizontal indicate the possible values of these convergent control parameters to gain a successful solution. Here, $\hbar$-curves have been drawn in Figs. 2 and 3 by taking $\hbar_F = \hbar_\Theta = \hbar_\Phi = \hbar$ horizontal axis versus $F''(0)$, $-\Theta'(0)$ and $-\Phi'(0)$. Accordingly, we have chosen for $\hbar_F = -0.866928, \hbar_\Theta = -0.726607$ and $\hbar_\Phi = -4.31526$ by implementing the code from BVPh2.0 package on Mathematica 12.1. Furthermore, from Fig. 4, we can see that, error reduced in a vertical axis as we roll up the order of approximation. Beside, Table 1 has been a testimony on successful accomplishment of convergence for $Ma = 0.5, Sc = Rn = 0.7, Nt = Nb = A = 0.3, Pr = 0.72, Ec = \Upsilon = 0.1$ with residual error on respective order of approximation. Pictorial representation of this table has been brought by Figs. 5, 6 and 7 for the value of $-F''(0)$, $-\Theta'(0)$ and $-\Phi'(0)$ in that order against the value of $n$ which attest getting the convergent values. Therefore, for this issue, HAM has been a guaranteed convergent solution with acceptable error.

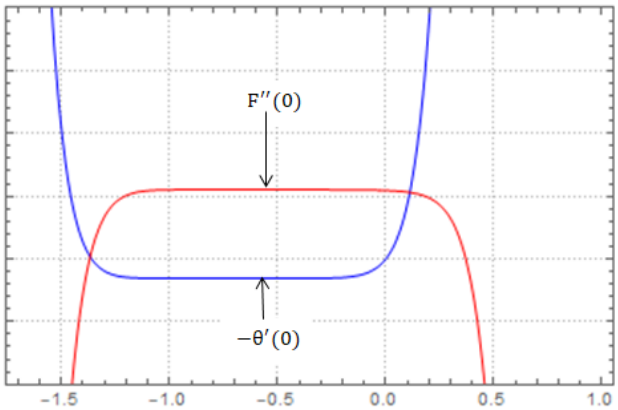


**Fig. 2** $\hbar$-curves for the convergence control parameters, $\hbar_F$ and $\hbar_\Theta$

## 4. COMPUTED OUTCOME AND DISCUSSION

The result of semi-analytic computations on this problem offered for velocity, temperature, nano-particle concentration, entropy and Benjan number with a brief discussion. These calculations have been done by HAM, which is running on the Mathematica 12.1 software with the BVPh2.0 package evolved by Zhao and Liao (2014). Graphical enlightenments have been given for the influence of incipient physical parameters on Eqs.

**Table 1** Order of approximation of HAM with Residual Error

| n | $m^{th}$ Order | $-F''(0)$ | $-\Theta'(0)$ | $-\Phi'(0)$ | Residual Error $-F''(0)$ | Residual Error $-\Theta'(0)$ | Residual Error $-\Phi'(0)$ |
|---|---|---|---|---|---|---|---|
| 1 | 7 | 1.31076 | 0.102848 | 0.802487 | | | |
| 2 | 9 | 1.31072 | 0.103012 | 0.801255 | | | |
| 3 | 10 | 1.3107 | 0.103058 | 0.801021 | $6.70 \times 10^{-11}$ | $4.31 \times 10^{-7}$ | $2.25 \times 10^{-8}$ |
| 4 | 12 | 1.3107 | 0.103118 | 0.800568 | $4.11 \times 10^{-12}$ | $1.37 \times 10^{-7}$ | $5.10 \times 10^{-9}$ |
| 5 | 15 | 1.3107 | 0.103159 | 0.800279 | | | |
| 6 | 18 | 1.3107 | 0.103176 | 0.800192 | $1.28 \times 10^{-15}$ | $4.82 \times 10^{-9}$ | $6.18 \times 10^{-11}$ |
| 7 | 21 | 1.3107 | 0.103184 | 0.800156 | | | |
| 8 | 24 | 1.3107 | 0.103187 | 0.800143 | $5.20 \times 10^{-19}$ | $1.78 \times 10^{-11}$ | $8.03 \times 10^{-13}$ |
| 9 | 27 | 1.3107 | 0.10319 | 0.80013 | | | |
| 10 | 30 | 1.3107 | 0.10319 | 0.80013 | $2.43 \times 10^{-22}$ | $6.66 \times 10^{-12}$ | $1.16 \times 10^{-14}$ |

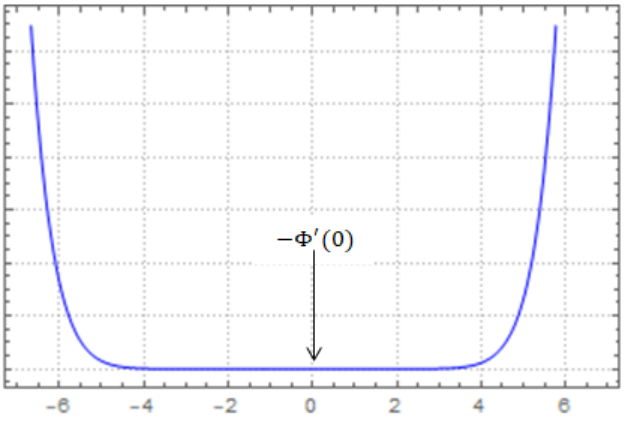


**Fig. 3** $\hbar$-curves for the convergence control parameters, $\hbar_\Phi$

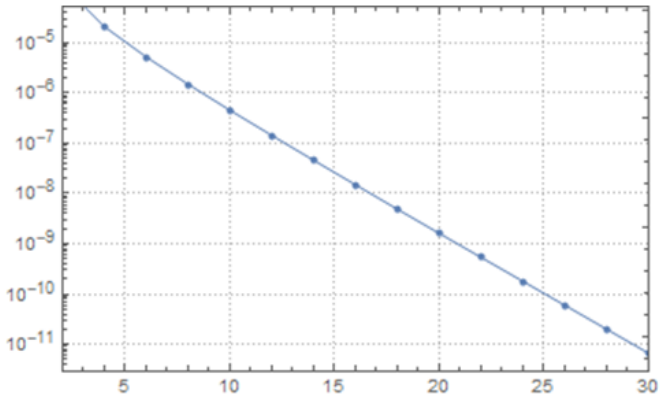


**Fig. 4** The order of approximation

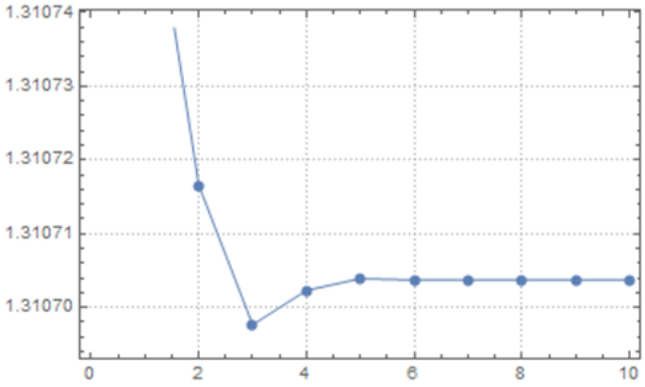


**Fig. 5** Convergence on the value of $-F''(0)$

(11) to (13) with boundary conditions in Eq. (14). Bearing in mind the nanofluids mobility as a working fluid, thermal radiation from the sunlight can be exchanged into heat energy for different purposes like preparing food, water warming, generating electricity, and so on. The validation of these computations have been justified by comparing the values of skin friction depending on $A$ with different previous published articles (Ullah *et al.* (2017); Bibi *et al.* (2018); Kebede *et al.* (2020)) as seen from Table 2. Additionally, Table 3 also lay out the covenant outcome of the existing solutions for distinct values of $Pr$ with Ullah *et al.* (2017), Aziz *et al.* (2021) and Anki Reddy *et al.* (2018).

**Table 2** Comparing the values of skin friction for different values of $A$

| $A$ | Ullah et al. ,2017 | Bibi et al. ,2018 | Kebede et al, ,2020 | **Present Result** |
|---|---|---|---|---|
| 0.1 | - | - | - | 1.034137 |
| 0.2 | - | 1.0685 | 1.06874 | 1.068027 |
| 0.3 | - | - | - | 1.101563 |
| 0.4 | - | 1.1349 | 1.13521 | 1.134657 |
| 0.5 | - | - | - | 1.167191 |
| 0.6 | - | 1.1992 | 1.19930 | 1.199148 |
| 0.7 | - | - | - | 1.23045 |
| 0.8 | 1.2610 | - | 1.26099 | 1.261102 |
| 1 | - | - | - | 1.32051 |
| 1.2 | 1.3777 | - | 1.37755 | 1.377705 |

### 4.1. Parameter's Repercussion on the Nanofluid Flow

The influence of magnetic field interaction on the movement of nanofluid alluded on Fig. 8. This outcome admitted with the fact that on stretching

**Table 3** Comparing the heat transfer rate for distinct values of $Pr$

| $Pr$ | Ullah et al. 2017 | Aziz et al, 2021 | Anki Reddy et al. 2018 | **Present Result** |
|---|---|---|---|---|
| 0.72 | 0.8088 | 0.8087618 | 0.80863 | 0.8086314 |
| 1 | 1 | 1 | 1 | 1.0 |
| 3 | 1.9237 | 1.923574 | 1.92368 | 1.9236826 |
| 7 | - | 3.07314651 | - | 3.0722474 |
| 10 | 3.7207 | 3.72055429 | 3.72060 | 3.7207112 |
| 20 | - | - | - | 5.3639140 |
| 30 | - | - | - | 6.6242008 |
| 50 | - | - | - | 8.6222647 |

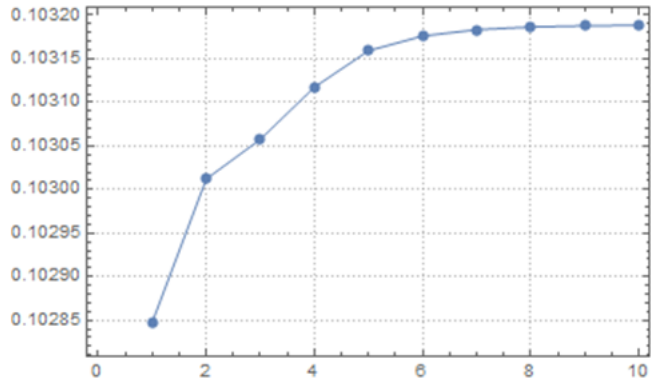


**Fig. 6** Convergence on the value of $-\Theta'(0)$

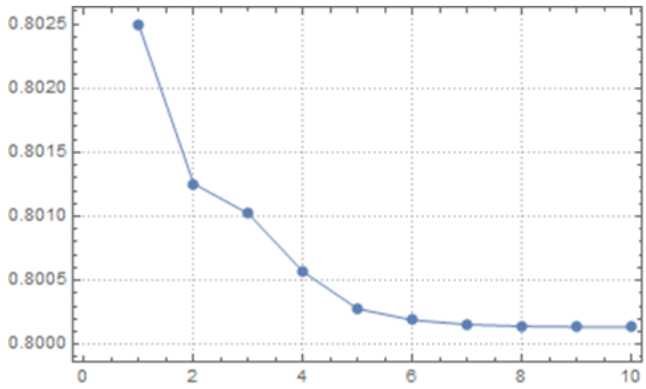


**Fig. 7** Convergence on the value of $-\Phi'(0)$

surface, the interaction of magnetic field generates Lorentz force which leads to rise up the drag like forces. As a consequence, the flow of a nanofluids retarded by this force which is realized pictorial in Fig. 8.

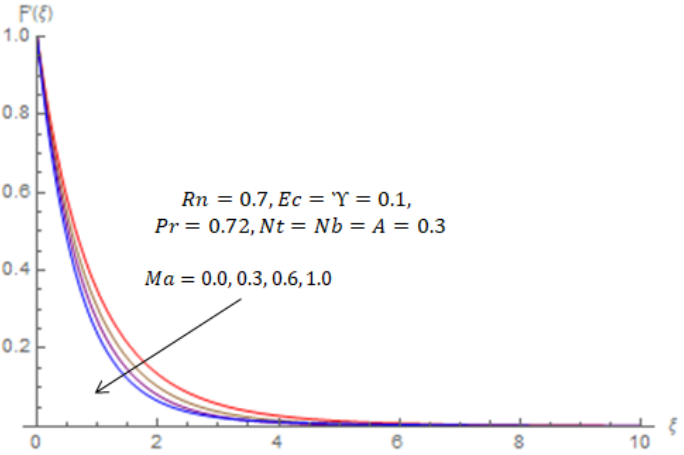


**Fig. 8** Impact of magnetic interaction parameter $Ma$ on $F'(\xi)$

### 4.2. Parameters' Repercussion on the Temperature Field

In energy Eq. (12), the parameters which are highly allied with dimensionless temperature are Ma, Rn, Ec, Pr and $\Upsilon$. The graphical representations from 9 to 13 are bespeaking the results obtained by executing HAM. Figure 9 marked that the temperature profile expands as the value of $Ma$ roll up. This is due to the production of heat as a byproduct of the viscous formation triggered by the maximum impedance of the nanofluids flow when the magnetic field mounts. The more heat generated by this viscous feature, the warmer the nanofluids as they travel. A byproduct of this circumstance leads to a wider temperature distribution. The impact of thermal radiation $Rn$ on dimensionless temperature field has been outlined in Fig. 10. Accordingly, $\Theta(\xi)$ grows up in accordance with $Rn$. This takes place due to the presence of more heat transfer from the solar radiations. Like $Rn$, temperature enlarges when Eckert number $Ec$ accrues according to Fig. 11. A non dimensional number $Ec$ represents the ratio of kinetic energy to entalpy variation in the boundary layer. From this point onward, whenever $Ec$ climbs, the kinetic energy also goes up, elevating the temperature of the nanofluids. Figure 12 flaunts the resultant of Biot numbr $\Upsilon$ on temperature. Boosting the heat transfer coefficient, which also elevates the value of $\Upsilon$, motivates expanding the temperature distribution. This is demystified by Fig. 12, where higher values of $\Upsilon$ propagate the temperature field. In another way, the distribution of temperature deducted as the Prantdl number $Pr$ augments what we have proved on Fig. 13. Based on the definition of Prantdl number, $Pr$ and thermal diffusivity are inversely related. This means that as $Pr$ tapers, the temperature of nanofluids rises.

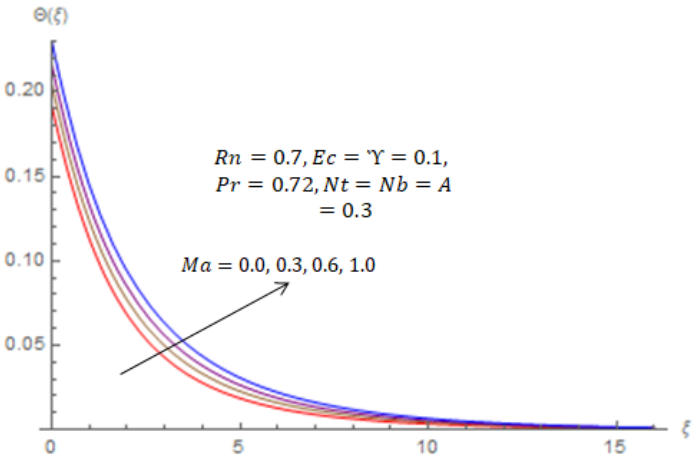


**Fig. 9** Impact of magnetic interaction parameter $Ma$ on $\Theta(\xi)$

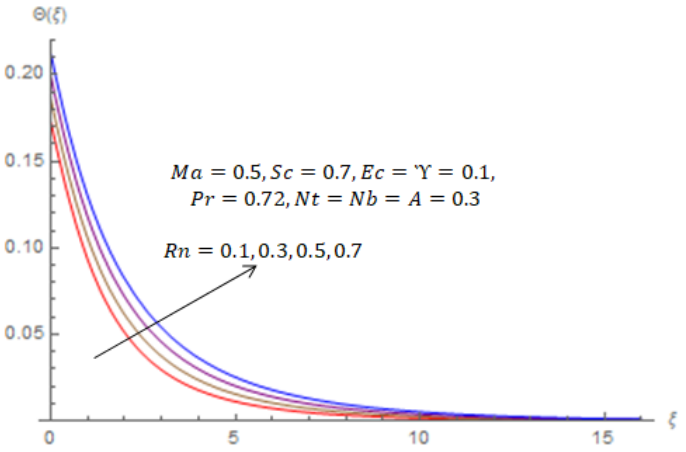


**Fig. 10** Impact of thermal radiation parameter $Rn$ on $\Theta(\xi)$

### 4.3. Parameters' Repercussion on the Concentration

The role of micro-sized solid particle concentrations on the heat and mass transfer through the flow of nanofluids in DASCs explicated by the prominent parameters such as Nt and Sc using the graph 14 and 15. From Fig. 14, it can be realized that the thermophoresis constant $Nt$ accelerates the

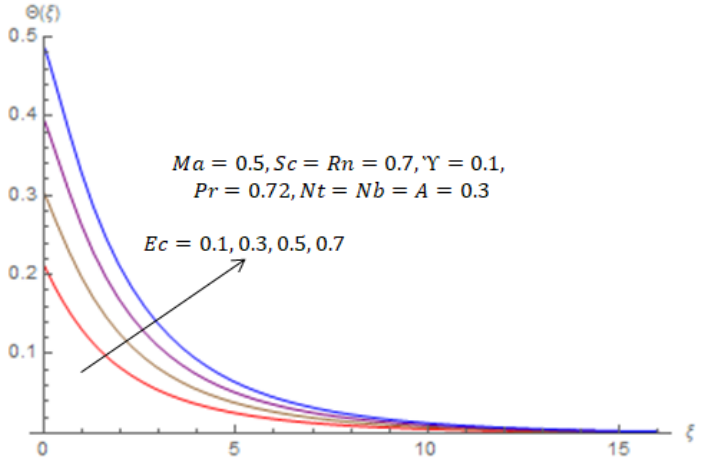


**Fig. 11** Impact of Eckert number $Ec$ on $\Theta(\xi)$

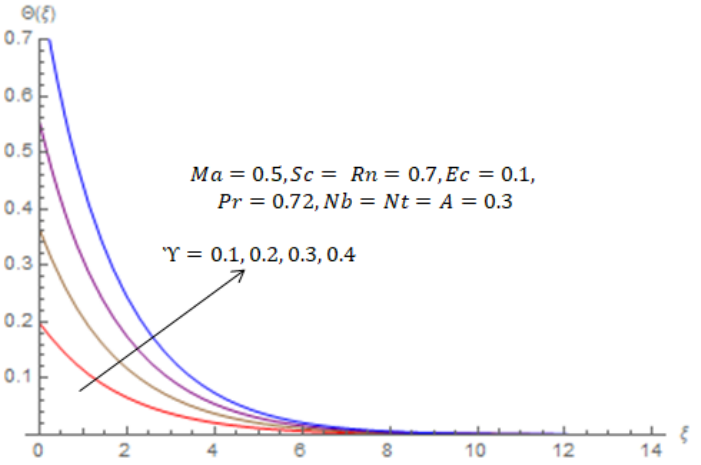


**Fig. 12** Impact of Biot number $\Upsilon$ on $\Theta(\xi)$

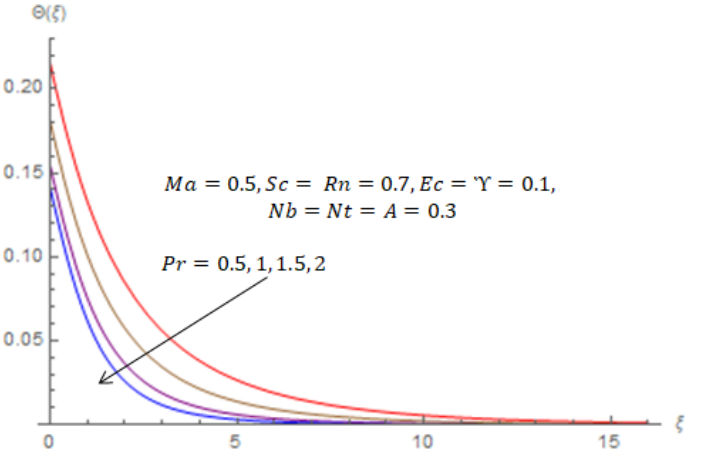


**Fig. 13** Impact of Prandtl number $Pr$ on $\Theta(\xi)$

micro-sized solid particle concentration. In this case, raising the values of $Nt$ enlarges the amount of $(\bar{T}_w - \bar{T}_\infty)$ which moves the small-sized particles from warm to cold. This results in adding the amount of nanoparticles concentration. The constant Schmidt number $Sc$ can be stated as the ratio of momentum diffusivity to mass diffusivity. The purpose of $Sc$ in convective mass transfer resembles to Prandtl number as in case of convective heat transfer. So, for more Schmidt number, the mass diffusivity abates, which causes the dropping of nanoparticle concentration as we inspected from Fig. 15.

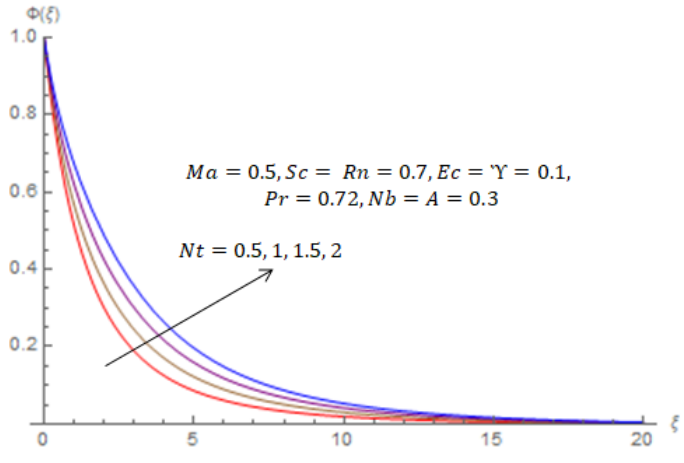


**Fig. 14** Impact of thermophoresis $Nt$ on $\Phi(\xi)$

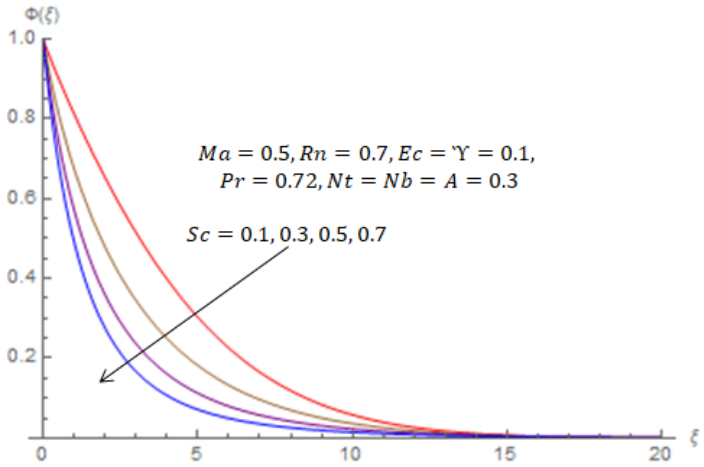


**Fig. 15** Impact of Schmidt number $Sc$ on $\Phi(\xi)$

### 4.4. Parameters' Repercussion on the Entropy and Bejan Number

In general, entropy has been generated due to irreversible actions, and its concept has been illuminated by thermodynamics second law for heat transfer. Based upon the contrived problem, the prominent parameters of entropy and also the Bejan number are $\Upsilon$, $Sc$ and $Ma$. Their spheres of influence have been revealed graphically from 16 to 18. Figure 16 pointed out that an accretion of $\Upsilon$ produces more entropy. The parameter $Ma$ promotes the production of entropy and also escalates the Bejan number, which ends up being near one, as we can see from Fig. 17. The findings on Figs. 16 and 17 are consistent with the published article quoted by Loganathan *et al.* (2021). Once the nanofluids discharge from the wall, the parameters $\Upsilon$ and $Ma$ exchange extra heat. In light of this, the entropy and Bejan numbers have gone up in that order. On the reverse side, a higher value of the Schmidt number $Sc$ diminutions the Bejan number, which is proved by Fig. 18. In general, the Bejan number is close to one at a distance.

### 4.5. Parameters' Repercussion on the Physical Quantities

This section explicates the impact of parameters on skin friction $Cf_x$, Nusselt number $Nu_x$ and Sherwood number $Sh_x$ defined in Eqs. (16), (18) and (19) taking $Re_x = 1$. Accordingly, the graph in Fig. 19 supported more accumulation of the skin friction coefficient $(-F''(0))$ when

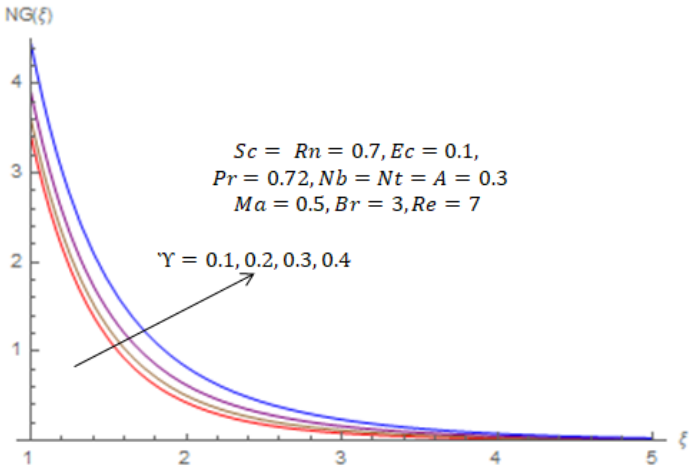


**Fig. 16** Impacts of $\Upsilon$ on non-dimensional entropy

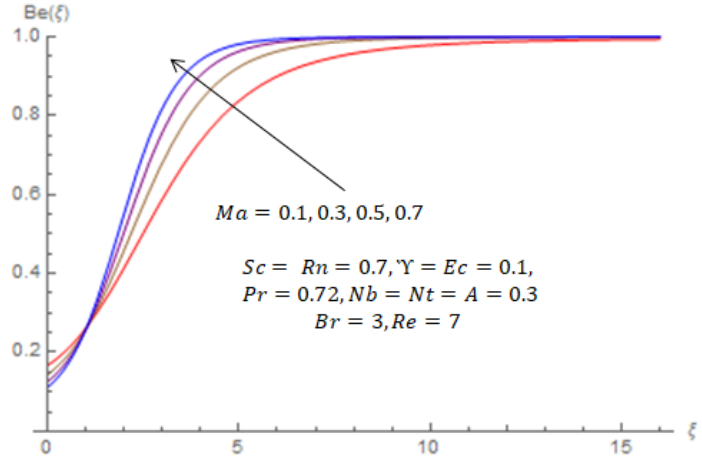


**Fig. 17** Impacts of $Ma$ on Bejan number

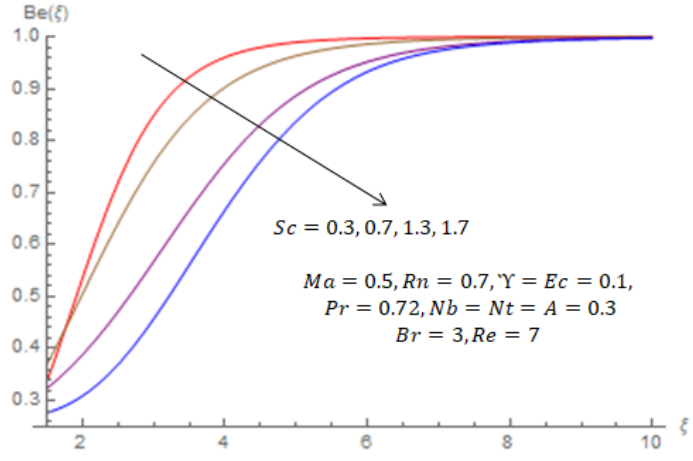


**Fig. 18** Impacts of $Sc$ on Bejan number

the value of $Ma$ has been high with a continuously increment of unsteadiness parameter $A$. Here, that is why these parameters lag the movement of nanofluids in D ASCs. The unsteadiness parameter $A$ keeps down the Nusselt number, whereas $Nt$ continuously escalates the heat transfer rate, as we saw in Fig. 20. This means that, the heat transfer rate grows with the thermophoresis constant and decelerates when time passes. By detracting $Ma$ and adding the value of $Nb$ without interruption, we intensify the Sherwood number, as we realized from Fig. 21.

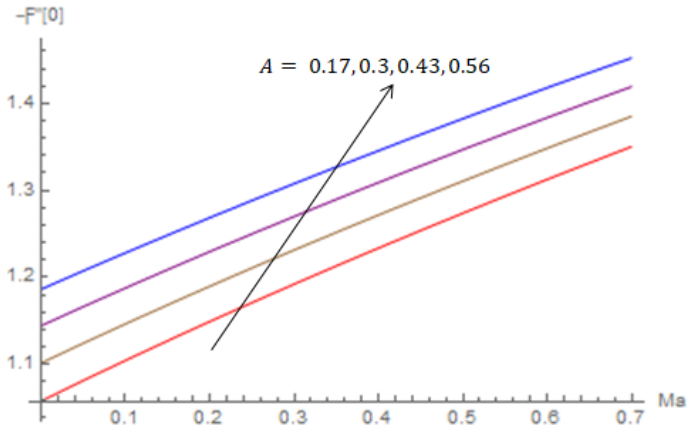


**Fig. 19** Impact of $A$ on $-F''(0)$ with $Ma$

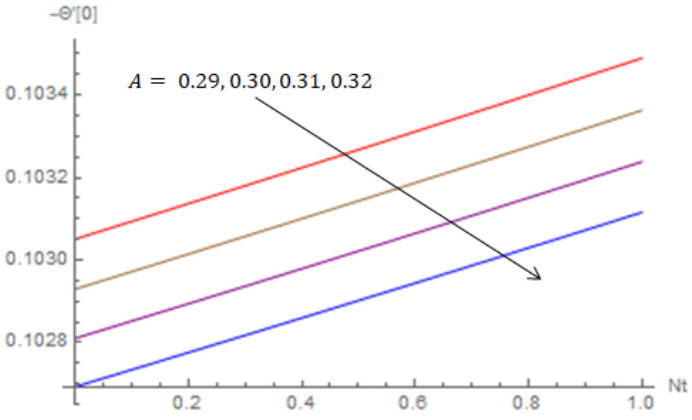


**Fig. 20** Impact of $A$ on $-\Theta'(0)$ with $Nt$

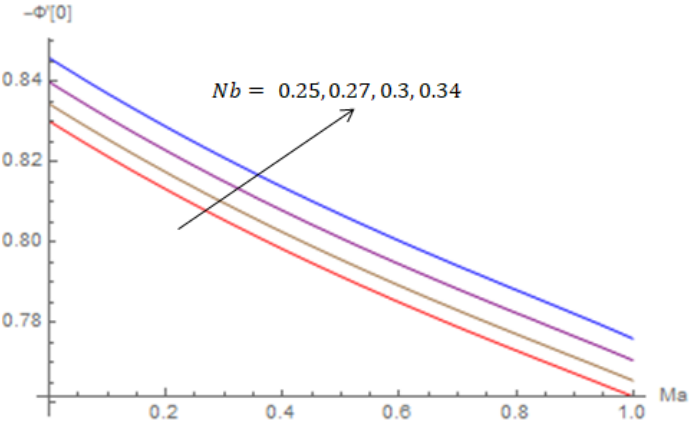


**Fig. 21** Impact of $Nb$ on$-\Phi'(0)$ with $Ma$

## 5. CONCLUSIONS

This work highlights the heat and mass transfer of incompressible, two-dimensional, time-dependent movable nanofluids across a DASC with the existence of renewable solar radiation and viscous dissipation. Entropy reproduction is also addressed in this aspect. Here, the nonlinear coupled higher-order systems of ODEs have been figured out by HAM after transforming the guiding PDEs into ODEs by similarity transformation. There upon, among many parameters that are actualized in this process,

Global Digital Central
ISSN: 2151-8629

the exceedingly influenced ones on dimensionless velocity, temperature, concentration of nanoparticle, and entropy have been demystified. The foremost upshot of this study has been wrapped up in the succeeding manner as a conclusion.

- Dimensionless velocity recedes as the value $Ma$ climbs.
- Accretion of $Ma$, $Rn$, $Ec$ and $\Upsilon$ upswings the temperature distribution while it dwindles as Prandtl number $Pr$ grows.
- The concentration of micro-sized particles proliferate for higher values of $Nt$ and wane away as $Sc$ becomes larger.
- There is a direct association between the entropy procreation and the value of $\Upsilon$. The Bejan number climbs with the ascending $Ma$ and descending $Sc$.
- The parameter $Ma$ and $A$ maximize the coefficient of skin friction in magnitude to which they retard the motion of nanofluids.
- Abating $A$ and picking up $Nt$, mounts the Nusselt number which, yields more heat transfer.
- The Sherwood number or mass transfer rate soars as the values of $Nb$ and $Ma$ elevates and abases, respectively.

## ACKNOWLEDGEMENTS

The researchers recognize with gratitude the reviewers insightful feedback and the authors of the literature studies cited in this paper for providing scientific aspects and ideas that supplement this work.

## NOMENCLATURE

| | |
|---|---|
| $\bar{C}$ | concentration (mol) |
| $\bar{T}$ | temperature (K) |
| $c_p$ | specific heat capacity (J/kg · K) |
| $H_f$ | convective heat transfer coefficient (W/K · m$^2$) |
| $k$ | thermal conductivity (kgm/s$^3$ · K) |
| $k^*$ | mean absorption coefficient (1/m) |
| $B_0$ | applied magnetic field (N/A · m$^2$) |
| $q_r$ | the rate of radiant energy emission (kg/s$^3$) |
| $D_B$ | Brownian motion coefficient (m$^2/s$) |
| $D_T$ | Thermophoretic diffusion coefficient (m$^2/s$) |
| $t$ | time (s) |
| $u_1$ | velocity along x axis (m/s) |
| $u_2$ | velocity along y axis (m/s) |
| $x, y$ | coordinate (m) |
| *Greek Symbols* | |
| $F$ | non-dimensional velocity |
| $\Theta$ | dimensionless temperature |
| $\Phi$ | non-dimensional concentration |
| $\psi$ | stream function m$^2/s$ |
| $\sigma^*$ | Stefan-Boltzmann constant (kg/s$^3$K$^4$) |
| $\rho$ | density (kg/m$^3$) |
| $\mu$ | diynamic viscousity (kg/ms) |
| $\nu$ | kinamatic (m$^2/s$) |
| $\tau$ | ratio of heat capacity |
| $\tau_w$ | shear wall stress (kg/ms$^2$) |
| $\sigma_e$ | electrical conductivity (s$^3A^2/(kg \cdot m)$) |
| *Subscripts* | |
| $w$ | wall |
| $\infty$ | ambient enviroment |

## REFERENCES

Al-Waeli, A.H., Sopian, K., Kazem, H.A., and Chaichan, M.T., 2017, "Photovoltaic/Thermal (PV/T) systems: Status and future prospects," *Renewable and Sustainable Energy Reviews*, **77**, 109–130. http://dx.doi.org/10.1016/j.rser.2017.03.126.

Alkathiri, A.A., Jamshed, W., Eid, M.R., Bouazizi, M.L., *et al.*, 2022, "Galerkin finite element inspection of thermal distribution of renewable solar energy in presence of binary nanofluid in parabolic trough solar collector," *Alexandria Engineering Journal*, **61**(12), 11063–11076. http://dx.doi.org/10.1016/j.aej.2022.04.036.

Anki Reddy, P.B., Reddy, S., and Suneetha, S., 2018, "Magnetohydro dynamic flow of blood in a permeable inclined stretching surface with viscous dissipation, non-uniform heat source/sink and chemical reaction," *Frontiers in Heat and Mass Transfer (FHMT)*, **10**. http://dx.doi.org/10.5098/hmt.10.22.

Azam, M., Shakoor, A., Rasool, H., and Khan, M., 2019, "Numerical simulation for solar energy aspects on unsteady convective flow of MHD Cross nanofluid: A revised approach," *International Journal of Heat and Mass Transfer*, **131**, 495–505. http://dx.doi.org/10.1016/j.ijheatmasstransfer.2018.11.022.

Aziz, A., Jamshed, W., and Aziz, T., 2018, "Mathematical model for thermal and entropy analysis of thermal solar collectors by using Maxwell nanofluids with slip conditions, thermal radiation and variable thermal conductivity," *Open Physics*, **16**(1), 123–136. http://dx.doi.org/10.1515/phys-2018-0020.

Aziz, A., Jamshed, W., Aziz, T., Bahaidarah, H., and Ur Rehman, K., 2021, "Entropy analysis of Powell–Eyring hybrid nanofluid including effect of linear thermal radiation and viscous dissipation," *Journal of Thermal Analysis and Calorimetry*, **143**(2), 1331–1343. http://dx.doi.org/10.1007/s10973-020-10210-2.

Bano, N., Singh, B., and Sayyed, S., 2018, "Homotopy analysis for MHD hiemenz flow in a porous medium with thermal radiation, velocity and thermal slips effects," *Frontiers in Heat and Mass Transfer (FHMT)*, **10**. http://dx.doi.org/10.5098/hmt.10.14.

Bayrak, F., Abu-Hamdeh, N., Alnefaie, K.A., and Öztop, H.F., 2017, "A review on exergy analysis of solar electricity production," *Renewable and Sustainable Energy Reviews*, **74**, 755–770. http://dx.doi.org/10.1016/j.rser.2017.03.012.

Bejan, A., 1996, "Entropy generation minimization: The new thermodynamics of finite-size devices and finite-time processes," *Journal of Applied Physics*, **79**(3), 1191–1218. http://dx.doi.org/10.1063/1.362674.

Bhalla, V., and Tyagi, H., 2017, "Solar energy harvesting by cobalt oxide nanoparticles, a nanofluid absorption based system," *Sustainable Energy Technologies and Assessments*, **24**, 45–54. http://dx.doi.org/10.1016/j.seta.2017.01.011.

Bhalla, V., and Tyagi, H., 2018, "Parameters influencing the performance of nanoparticles-laden fluid-based solar thermal collectors: a review on optical properties," *Renewable and Sustainable Energy Reviews*, **84**, 12–42. http://dx.doi.org/10.1016/j.rser.2017.12.007.

Bibi, M., Malik, M., Tahir, M., *et al.*, 2018, "Numerical study of unsteady Williamson fluid flow and heat transfer in the presence of MHD through a permeable stretching surface," *The European Physical Journal Plus*, **133**(4), 1–15. http://dx.doi.org/10.1140/epjp/i2018-11991-2.

Brewster, M.Q., 1992, *Thermal radiative transfer and properties*, John Wiley & Sons.

Buongiorno, J., 2006, "Convective transport in nanofluids," http://dx.doi.org/10.1115/1.2150834.

Choi, S.U., and Eastman, J.A., 1995, "Enhancing thermal conductivity of fluids with nanoparticles," Tech. rep., Argonne National Lab.(ANL), Argonne, IL (United States).

Daniel, Y.S., Aziz, Z.A., Ismail, Z., and Salah, F., 2017, "Entropy analysis in electrical magnetohydrodynamic (MHD) flow of nanofluid with effects of thermal radiation, viscous dissipation, and chemical reaction," *Theoretical and Applied Mechanics Letters*, **7**(4), 235–242. http://dx.doi.org/10.1016/j.taml.2017.06.003.

Dincer, I., 2000, "Renewable energy and sustainable development: a crucial review," *Renewable and sustainable energy reviews*, **4**(2), 157–175. http://dx.doi.org/10.1016/S1364-0321(99)00011-8.

Dugaria, S., Bortolato, M., and Del Col, D., 2018, "Modelling of a direct absorption solar receiver using carbon based nanofluids under concentrated solar radiation," *Renewable Energy*, **128**, 495–508. http://dx.doi.org/10.1016/j.renene.2017.06.029.

Everett, R., Boyle, G., Peake, S., and Ramage, J., 2012, *Energy systems and sustainability: power for a sustainable future*, Oxford Univerity Press.

Flilihi, E., Sebbar, E., Achemlal, D., EL Rhafiki, T., Sriti, M., and Chaabelasri, E., 2022, "Effect of absorber design on convective heat transfer in a flat plate solar collector: A CFD modeling," *Frontiers in Heat and Mass Transfer (FHMT)*, **18**. http://dx.doi.org/10.5098/hmt.18.39.

Gorji, T.B., and Ranjbar, A., 2017, "A review on optical properties and application of nanofluids in direct absorption solar collectors (DASCs)," *Renewable and Sustainable Energy Reviews*, **72**, 10–32. http://dx.doi.org/10.1016/j.rser.2017.01.015.

Hayat, T., Riaz, R., Aziz, A., and Alsaedi, A., 2019, "Analysis of entropy generation for MHD flow of third grade nanofluid over a nonlinear stretching surface embedded in a porous medium," *Physica Scripta*, **94**(12), 125703. http://dx.doi.org/10.1088/1402-4896/ab3308.

Hayat, T., Ullah, I., Muhammad, K., and Alsaedi, A., 2021, "Gyrotactic microorganism and bio-convection during flow of Prandtl-Eyring nanomaterial," *Nonlinear Engineering*, **10**(1), 201–212. http://dx.doi.org/10.1515/nleng-2021-0015.

Hussain, S.M., 2022, "Dynamics of radiative Williamson hybrid nanofluid with entropy generation: significance in solar aircraft," *Scientific Reports*, **12**(1), 1–23. http://dx.doi.org/10.1038/s41598-022-13086-4.

Hussain, T., Hayat, T., Shehzad, S.A., Alsaedi, A., and Chen, B., 2015, "A model of solar radiation and Joule heating in flow of third grade nanofluid," *Zeitschrift für Naturforschung A*, **70**(3), 177–184. http://dx.doi.org/10.1515/zna-2014-0267.

Jamshed, W., Eid, M.R., Nasir, N.A.A.M., Nisar, K.S., Aziz, A., Shahzad, F., Saleel, C.A., and Shukla, A., 2021, "Thermal examination of renewable solar energy in parabolic trough solar collector utilizing Maxwell nanofluid: A noble case study," *Case Studies in Thermal Engineering*, **27**, 101258. http://dx.doi.org/10.1016/j.csite.2021.101258.

Kebede, T., Haile, E., Awgichew, G., and Walelign, T., 2020, "Heat and mass transfer in unsteady boundary layer flow of Williamson nanofluids," *Journal of Applied Mathematics*, **2020**. http://dx.doi.org/10.1155/2020/1890972.

Lei, W., Ozturk, I., Muhammad, H., and Ullah, S., 2022, "On the asymmetric effects of financial deepening on renewable and non-renewable energy consumption: insights from China," *Economic Research-Ekonomska Istraživanja*, **35**(1), 3961–3978. http://dx.doi.org/10.1080/1331677X.2021.2007413.

Liao, S.J., 1992, *The proposed homotopy analysis technique for the solution of nonlinear problems*, Ph.D. thesis, PhD thesis, Shanghai Jiao Tong University.

Loganathan, K., Mohana, K., Mohanraj, M., Sakthivel, P., and Rajan, S., 2021, "Impact of third-grade nanofluid flow across a convective surface in the presence of inclined Lorentz force: an approach to entropy optimization," *Journal of Thermal Analysis and Calorimetry*, **144**(5), 1935–1947. http://dx.doi.org/10.1007/s10973-020-09751-3.

Loganathan, K., and Rajan, S., 2020, "An entropy approach of Williamson nanofluid flow with Joule heating and zero nanoparticle mass flux," *Journal of Thermal Analysis and Calorimetry*, **141**(6), 2599–2612. http://dx.doi.org/10.1007/s10973-020-09414-3.

Maouassi, A., Baghidja, A., Douad, S., and Zeraibi, N., 2018, "Heat exchanges intensification through a flat plat solar collector by using nanofluids as working fluid," *Frontiers in Heat and Mass Transfer (FHMT)*, **10**. http://dx.doi.org/10.5098/hmt.10.35.

Minardi, J.E., and Chuang, H.N., 1975, "Performance of a "black" liquid flat-plate solar collector," *Solar Energy*, **17**(3), 179–183. http://dx.doi.org/10.1016/0038-092X(75)90057-2.

Pandey, K.M., and Chaurasiya, R., 2017, "A review on analysis and development of solar flat plate collector," *Renewable and Sustainable Energy Reviews*, **67**, 641–650. http://dx.doi.org/10.1016/j.rser.2016.09.078.

Panwar, N., Kaushik, S., and Kothari, S., 2011, "Role of renewable energy sources in environmental protection: A review," *Renewable and sustainable energy reviews*, **15**(3), 1513–1524. http://dx.doi.org/10.1016/j.rser.2010.11.037.

Rafique, K., Anwar, M.I., Misiran, M., Khan, I., Alharbi, S., Thounthong, P., and Nisar, K., 2019, "Numerical solution of casson nanofluid flow over a non-linear inclined surface with soret and dufour effects by keller-box method," *Frontiers in Physics*, **7**, 139. http://dx.doi.org/10.3389/fphy.2019.00139.

Rasheed, H.U., Islam, S., Helmi, M.M., Alsallami, S.A., Khan, Z., and Khan, I., 2021, "An analytical study of internal heating and chemical reaction effects on MHD flow of nanofluid with convective conditions," *Crystals*, **11**(12), 1523. http://dx.doi.org/10.3390/cryst11121523.

Rasih, R.A., Sidik, N.A.C., and Samion, S., 2019, "Recent progress on concentrating direct absorption solar collector using nanofluids," *Journal of Thermal Analysis and Calorimetry*, **137**(3), 903–922. http://dx.doi.org/10.1007/s10973-018-7964-6.

Sabiha, M., Saidur, R., Mekhilef, S., and Mahian, O., 2015, "Progress and latest developments of evacuated tube solar collectors," *Renewable and Sustainable Energy Reviews*, **51**, 1038–1054. http://dx.doi.org/10.1016/j.rser.2015.07.016.

Saeed, A., Algehyne, E.A., Aldhabani, M.S., Dawar, A., Kumam, P., and Kumam, W., 2022, "Mixed convective flow of a magnetohydrodynamic Casson fluid through a permeable stretching sheet with first-order chemical reaction," *Plos one*, **17**(4), e0265238.
http://dx.doi.org/10.1371/journal.pone.0265238.

Sathe, T.M., and Dhoble, A., 2017, "A review on recent advancements in photovoltaic thermal techniques," *Renewable and Sustainable Energy Reviews*, **76**, 645–672.
http://dx.doi.org/10.1016/j.rser.2017.03.075.

Sathyamurthy, R., Nagarajan, P., Kennady, H., Ravikumar, T., Paulson, V., and Ahsan, A., 2014, "Enhancing the heat transfer of triangular pyramid solar still using phase change material as storage material," *Frontiers in Heat and Mass Transfer (FHMT)*, **5**(1).
http://dx.doi.org/10.5098/hmt.5.3.

Smit, S., and Kessels, W., 2015, "Variational method for the minimization of entropy generation in solar cells," *Journal of Applied Physics*, **117**(13), 134504.
http://dx.doi.org/10.1063/1.4916787.

Statistics, E., 2016, "Ministry of Statistics and Programme Implementation Government of India,"
http://dx.doi.org/10.1016/j.rser.2017.03.126.

Subramani, J., Nagarajan, P., Mahian, O., and Sathyamurthy, R., 2018, "Efficiency and heat transfer improvements in a parabolic trough solar collector using TiO2 nanofluids under turbulent flow regime," *Renewable energy*, **119**, 19–31.
http://dx.doi.org/10.1016/j.renene.2017.11.079.

Szulejko, J.E., Kumar, P., Deep, A., and Kim, K.H., 2017, "Global warming projections to 2100 using simple CO2 greenhouse gas modeling and comments on CO2 climate sensitivity factor," *Atmospheric Pollution Research*, **8**(1), 136–140.
http://dx.doi.org/10.1016/j.apr.2016.08.002.

Tiwari, G.N., and Mishra, R.K., 2012, *Advanced renewable energy sources*, Royal Society of Chemistry.

Tyagi, S., Wang, S., Singhal, M., Kaushik, S., and Park, S., 2007, "Exergy analysis and parametric study of concentrating type solar collectors," *International journal of thermal sciences*, **46**(12), 1304–1310.
http://dx.doi.org/10.1016/j.ijthermalsci.2006.11.010.

Ullah, I., Khan, I., and Shafie, S., 2017, "Soret and Dufour effects on unsteady mixed convection slip flow of Casson fluid over a nonlinearly stretching sheet with convective boundary condition," *Scientific Reports*, **7**(1), 1–19.
http://dx.doi.org/10.1038/s41598-017-01205-5.

Van Gorder, R.A., 2014, "Chapter 4: Stability of Auxiliary Linear Operator and Convergence-Control Parameter in the Homotopy Analysis Method," *Advances in the Homotopy Analysis Method*, 123–180, World Scientific.

Wakif, A., Boulahia, Z., Amine, A., Animasaun, I., Afridi, M., Qasimd, M., and Sehaqui, R., 2018, "Magneto-convection of alumina-water nanofluid within thin horizontal layers using the revised generalized Buongiorno's model," *Frontiers in Heat and Mass Transfer (FHMT)*, **12**.
http://dx.doi.org/10.5098/hmt.12.3.

Zhao, Y., and Liao, S., 2014, "Chapter 9: HAM-Based Mathematica Package BVPh 2.0 for Nonlinear Boundary Value Problems," *Advances in the homotopy analysis method*, 361–417, World Scientific.